THE JOURNAL OF BIOLOGICAL CHEMISTRY VOL. 289, NO. 2, pp. 778–788, January 10, 2014

Structural Basis for Inflammation-driven Shedding of CD163 Ectodomain and Tumor Necrosis Factor-α in Macrophages*

Received for publication, September 18, 2013, and in revised form, November 21, 2013 Published, JBC Papers in Press, November 25, 2013, DOI 10.1074/jbc.M113.520213

Anders Etzerodt[‡], Mie Rostved Rasmussen[‡], Pia Svendsen[‡], Athena Chalaris[§], Jeanette Schwarz[§], Ian Galea[¶], Holger Jon Møller[‖], and Søren Kragh Moestrup[‡‖1]

From the [‡]Department of Biomedicine, Aarhus University, DK-8000 Aarhus C, Denmark, the [§]Department of Biochemistry, Christian-Albrechts-Universität zu Kiel, 24118 Kiel, Germany, the [¶]Clinical and Experimental Sciences, Faculty of Medicine, University of Southampton, Southampton SO17 1BJ, United Kingdom, and the [‖]Department of Clinical Biochemistry, Aarhus University Hospital, DK-8000 Aarhus C, Denmark

Background: ADAM17 mediates shedding of CD163 and tumor necrosis factor-α (TNF-α) during inflammation.
Results: Similar substrate sequence motifs in proTNF-α and CD163 are essential for ADAM17-mediated cleavage.
Conclusion: The structural basis for shedding of CD163 and TNF-α is disclosed.
Significance: The data provide new molecular information on the inflammatory response and explain evolution of a regulatory mechanism for CD163 expression.

The haptoglobin-hemoglobin receptor CD163 and proTNF-α are transmembrane macrophage proteins subjected to cleavage by the inflammation-responsive protease ADAM17. This leads to release of soluble CD163 (sCD163) and bioactive TNF-α. Sequence comparison of the juxtamembrane region identified similar palindromic sequences in human CD163 (^{1044}Arg-Ser-Ser-Arg) and proTNF-α (^{78}Arg-Ser-Ser-Ser-Arg). In proTNF-α the Arg-Ser-Ser-Ser-Arg sequence is situated next to the previously established ADAM17 cleavage site. Site-directed mutagenesis revealed that the sequences harbor essential information for efficient cleavage of the two proteins upon ADAM17 stimulation. This was further evidenced by analysis of mouse CD163 that, like CD163 in other non-primates, does not contain the palindromic CD163 sequence in the juxtamembrane region. Mouse CD163 resisted endotoxin- and phorbol ester-induced shedding, and *ex vivo* analysis of knock-in of the Arg-Ser-Ser-Arg sequence in mouse CD163 revealed a receptor shedding comparable with that of human CD163. In conclusion, we have identified an essential substrate motif for ADAM17-mediated CD163 and proTNF-α cleavage in macrophages. In addition, the present data indicate that CD163, by incorporation of this motif in late evolution, underwent a modification that allows for an instant down-regulation of surface CD163 expression and inhibition of hemoglobin uptake. This regulatory modality seems to have coincided with the evolution of an enhanced hemoglobin-protecting role of the haptoglobin-CD163 system in primates.

ADAM17,[2] alias TNF-α-converting enzyme, belongs to the "a disintegrin and metalloproteinase (ADAM)" family of transmembrane proteases. It has a multi-substrate specificity, and it is involved in several cellular processes such as cytokine, hormone, and growth factor release (1). ADAM17-dependent shedding is also involved in regulated intramembrane proteolysis releasing cytoplasmic mediators and in inhibition of extracellular signaling and ligand uptake by a rapid down-regulation of surface receptors. Because of the many different substrates of ADAM17, the protein has a key role in both homeostatic and pathologic processes (2). ADAM17 is widely known for its activation of macrophage TNF-α by cleavage of membrane-bound proTNF-α (3, 4), and as a consequence, it is designated TNF-α-converting cleavage enzyme. TNF-α is one of the most potent proinflammatory cytokines known, which indicates an indirect proinflammatory role of ADAM17 in inflammatory macrophages (2, 5). proTNF-α, which is a homotrimeric type II transmembrane protein (N terminus in the cytoplasmic tail), is cleaved by ADAM17 between Ala^{76} and Val^{77} (^{76}A ↓ V) in the juxtamembrane region (3, 4, 6).

In accordance with promotion of the proinflammatory state in macrophages, ADAM17 was also recently shown to cleave and thereby down-regulate the surface expression of the hemoglobin scavenger receptor CD163 (7). This receptor is suggested to serve an anti-inflammatory function by clearance of the extracellular haptoglobin-hemoglobin complexes and the heme oxygenase-mediated conversion of proinflammatory heme to anti-inflammatory heme metabolites (8, 9). The ADAM17-mediated cleavage leads to generation of soluble CD163 (sCD163), a byproduct that is highly up-regulated in plasma during infectious and inflammatory conditions (7, 10). CD163 is a type I transmembrane protein with an opposite orientation as compared with proTNF-α. The ADAM17-dependent cleavage of the CD163 ectodomain occurs in the juxtamembrane region in an as yet unidentified cleavage site and results in shedding of the sCD163 ectodomain, consisting of nine SRCR domains (11, 12).

In contrast to TNF-α, which is almost absent in normal plasma, sCD163 is present in a rather high concentration (1–4 mg/liter) (12). Upon proinflammatory stimulation the plasma

* This work was supported by grants from the Danish Medical Research Council, the Novo Nordisk Foundation, the European Research Council (Advanced Grant for the TROJA program, Grant 233312), and the Lundbeck Foundation.
[1] To whom correspondence should be addressed: Dept. of Biomedicine, Aarhus University, Ole Worms Alle 3, DK-8000 Aarhus C, Denmark. Tel.: 45-28992282; E-mail: skm@biokemi.au.dk.
[2] The abbreviations used are: ADAM17, a disintegrin and metalloproteinase-17; MBDM, mouse bone marrow-derived macrophage; sCD163, soluble CD163; hCD163, human CD163; mCD163, mouse CD163; SRCR, scavenger receptor cysteine-rich; TIMP3, tissue inhibitor of metalloproteinases-3; PMA, phorbol 12-myristate 13-acetate.

level of both proteins is rapidly elevated. This was recently demonstrated in a human study of experimental endotoxemia where a bolus injection of LPS caused a fast and simultaneous increase of TNF-α and sCD163 (7). Both proteins peaked after 1.5 h, but although TNF-α was no longer detectable in circulation after 3 h, the LPS-induced increase in sCD163 persisted for more than 24 h. In line with this an elevated level of sCD163 is reported in patients suffering from various infectious and inflammatory diseases such as sepsis, tuberculosis, diabetes, human immunodeficiency virus, rheumatoid arthritis, and hemophagocytosis (13).

The physiological role, if any, of sCD163 is so far unknown, but it has been speculated that release of sCD163 and subsequent formation of an sCD163-haptoglobin-hemoglobin complex may suppress the heme iron supply to hemolytic bacteria and trypanosomes (14, 15). Moreover sCD163 has been suggested to inhibit activated T lymphocyte proliferation and recently also to promote recognition and phagocytosis of *Staphylococcus aureus* (16, 17).

CD163 is expressed in all mammalian species, and the human protein displays more than 71% amino acid similarity to its reported orthologs including chimpanzee, green monkey, swine, dog, cow, rat, and mouse CD163. Despite the very high amino acid similarity, the mechanism of haptoglobin-mediated hemoglobin scavenging differs substantially between mice (18) and humans (19). In humans, efficient uptake of hemoglobin via the CD163 system requires preformation of the haptoglobin-hemoglobin complex, whereas mouse CD163 efficiently mediates uptake of hemoglobin independent of haptoglobin-hemoglobin complex formation.

To define the molecular basis for ADAM17-mediated cleavage of CD163, we have now made a comparative mutagenesis analysis of proTNF-α and CD163 cleavage in mice and humans. This led to identification of a common motif for ADAM17-mediated cleavage of the two protein humans and the surprising finding that inflammation-driven down-regulation of CD163 by ADAM17-mediated cleavage seems specific for primate species.

EXPERIMENTAL PROCEDURES

Materials—Rat monoclonal (mAb) anti-mouse CD163 (3E10B10) used earlier (20) was a kind gift from Cytoguide ApS (Aarhus Denmark). Biotinylated E10B10 was prepared by incubating antibody with Biotin-NHS (Sigma-Aldrich, Copenhagen, Denmark) in 40× molar excess at pH 8.5. Excess biotin was subsequently removed by dialysis against 1× PBS, pH 7.4, overnight at 4 °C. Rabbit polyclonal (pAb) anti-mouse CD163 was directed against recombinant mouse CD163 SRCR domain 1–9 (Dako Denmark A/S, Glostrup, Denmark) (18). Phorbol 12-myristate 13-acetate (PMA) and lipopolysaccharide (LPS, serotype 0111:B4) were from Sigma-Aldrich, and mouse macrophage colony-stimulating factor (M-CSF) were from Life Technologies (Life Technologies Europe BV, Naerum, Denmark). Human CD163 (hCD163) cDNA (7) and mouse CD163 (mCD163) cDNA (18) were used earlier. cDNA encoding human proTNF-α and the proTNF-α ^{78}RS/AA mutant were synthesized by GenScript (GenScript USA Inc., Piscataway, NJ) using GenBank™ accession number M10988.1 as template.

Cell Culture and Knockdown of ADAM17—Transfected human embryonic kidney cells expressing either mCD163 or hCD163 or variants thereof were established as described earlier using the FlpIn system (Life Technologies, Taastrup, Denmark) (7). Knockdown of ADAM17 and subsequent semiquantitative RT-PCR analysis were done as described previously (7). Murine bone marrow-derived macrophages (MBDMs) were prepared by harvesting femurs and tibias from 8-week-old C57BL/6NTac mice, and bone marrow was collected using the method described in Ref. 21. Freshly collected bone marrow cells were resuspended at 6×10^5 cells/ml in RPMI 1640 supplemented with 10% FCS, 2 mM L-glutamine, and 25 ng/ml M-CSF. Cells were cultured for 7 days and subsequently used as described.

Cellular shedding of CD163 was induced by 1 h of incubation at 37 °C in PBS, pH 7.4, with or without 100 ng/ml PMA or, where indicated, with a gradient of 10^0 to 10^5 ng/ml PMA. MBDMs were incubated with 25 ng/ml LPS or 100 ng/ml PMA in complete growth medium for 4 h at 37 °C. Where specified, cells were preincubated with 250 nM TIMP3 inhibitor for 30 min at 37 °C (Sigma-Aldrich).

ELISA, Western Blotting, and Image Cytometry—TNF-α was measured by a commercial ELISA kit (mouse TNF-α Instant ELISA, eBioscience, Frankfurt, Germany). Mouse sCD163 was measured by a sandwich ELISA assay using rabbit pAb anti-mouse CD163 as capture antibody and biotinylated E10B10 as detection antibody. In short, capture antibody was diluted to 2 μg/ml in PBS, pH 7.4, and incubated overnight at 4 °C in microtiter plates (Nunc MaxiSorp, Nunc A/S, Roskilde, Denmark). Wells were blocked in 25 g/liter casein for 2 h at room temperature and washed with PBST (1× PBS, pH 7.4, 0.5 mM NaCl, 0,1% Tween 20). The samples were diluted in 25 g/liter casein and incubated in plates for 2 h at room temperature. The concentration of detection antibody was 1 μg/ml. Antibody-antigen complexes were visualized by horseradish peroxidase (HRP)-conjugated streptavidin (Sigma-Aldrich) and a ready-to-use solution of 3,3′, 5,5′-tetramethylbenzidine (Life Technologies). Enzyme reaction was quenched with 1 M H_3PO_4, and absorbance was read at 450 nm in a microplate reader (VersaMax microplate reader, Molecular Devices Ltd., Hampshire, UK). Mouse CD163 SRCR domain 1–9 was used as a calibrator (protein standard) and was expressed and purified as described previously (18). Human sCD163 was measured by a previously established ELISA assay (22). Western blotting of sCD163 was carried out using rabbit pAb anti-mouse CD163 and a secondary HRP-conjugated goat anti-rabbit IgG antibody (Sigma-Aldrich). Immunoreactive bands were visualized on a FUJI FLA3000 Gel Doc (Fujifilm Europe GmbH, Düsseldorf, Germany) using an ECL substrate (Pierce) and a 240-s exposure time. Intensities of immunoreactive bands were quantified using the MultiGauge software (Fujifilm Europe GmbH). Cells for image cytometry were prepared as described previously (23) using ATTO488-conjugated rabbit pAb anti-mouse CD163 antibody. Cells were analyzed on a Nucleoview NC-3000 FlexiCyte image cytometer (Chemometec A/S). Image cytometry data were analyzed by FCS Express version 4.0 (De Novo Software, Los Angeles, CA).

Generation of CD163 Mutants and Chimeras—The human CD163 mutants (hCD163^{1044}RS/AA and hCD163^{1046}SR/AA), the mouse CD163 mutant (mCD163 RSSR) and the juxtamembrane chimeras (hCD163mjux, mCD163hjux) were prepared using the Site-directed, Ligase-Independent Mutagenesis (SLIM) method (24). The mouse CD163 chimeras (mCD163chim1–4) were constructed using an overlap extension PCR method (25). Templates for the PCR reactions consisted of the pcDNA5/FRT plasmid containing either human CD163 cDNA or mouse CD163 cDNA. Primers for hCD163 RS/AA were: F_S, 5′-TCCTTTATTGCAGTCGGG, R_S, 5′-ACCTGTTGTGGCTTTTTG, F_T, 5′-CGCTCAGCCGCACAGTCATCCTTTATTGCAGTCGGG, R_T, 5′-TGACTGTGCGGCTGAGCGACCTGTTGTGCCTTTTTG. Primers for hCD163 SR/AA were: F_S, 5′-TCCTTTATTGCAGTCGGG, R_S, 5′-ACCTGTTGTGGCTTTTTG, F_T, 5′-GCCGCATCCCGTCAGTCATCCTTTATTGCAGTCGGG, R_T, 5′-TGACTGACGGGATGCGGCACCTGTTGTGGCTTTTTG. Primers for mCD163 RSSR were: F_S, 5′-CACCCCACCCTCACGGCA, R_S, 5′-ACCTGTGCCATGATGTGA, F_T, 5′-CGCTCATCCCGTCACCCCACCCTCACGGCA, R_T, 5′-ACGGGATGAGCGACCTGTGCCATGATGTGA. Primers for hCD163mjux were: F_S, 5′-TTTATTGCAGTCGGGATC, R_S, 5′-TGTGCAATTCACTGCAGC, F_T, 5′-GAATCACACATGGCACAGGTCACCCCACCTTTATTGCAGTCGGGATC, R_T, 5′-TGTGCCATGATGTGATTCTGAAGTCATTTTTGGTGTGCAATTCACTGCAGC. Primers for mCD163hjux were: F_S, 5′-CTCACGGCACTCTTGGTT, R_S, 5′-GAGGCACTGGATGGAAGC, F_T, 5′-CCACAAAAAGCCACAACAGGTCGCTCATCCCGTCAGTCATCCCTCACGGCACTCTTGGTT, R_T, 5′-TGTTGTGGCTTTTTGTGGGGTTTCTGCACTGAAATATCGAGGCACTGGATGGAAGC. Primers for mCD163chim1 were: PA_S, 5′-GAGGGTACCATGGGTGGACACAGAATG, PA_r, 5′-CTGAAGTCTTATCTTGTTGTCACAGATGATCCAGGACTC, PB_s, 5′-TCCTGGATCATCTGTGACAACAAGATAAGACTTCAGGAA, PB_r, 5′-GAGCTCGAGTCACTGGGTTATAAATTC. Primers for mCD163chim2 were: PA_S, 5′-GAGGGTACCATGGGTGGACACAGAATG, PA_r, 5′-TTTCTGCACTGAAATATCGAGGCACTGGATGGAAGCATC, PB_s, 5′-GCTTCCATCCAGTGCCTCGATATTTCAGTGCAGAAAACC, PB_r, 5′-GAGCTCGAGTCACTGGGTTATAAATTC. Primers for mCD163chim3 were: PA_S, 5′-GAGGGTACCATGGGTGGACACAGAATG, PA_r, 5′-GATCCCGACTGCAATAAAGGTGGGGTGACCTGTGCCATG, PB_s, 5′-GGCACAGGTCACCCCACCTTTATTGCAGTCGGGATCCTT, PB_r, 5′-GAGCTCGAGTCACTGGGTTATAAATTC. Primers for mCD163chim4 were: PA_S, 5′-GAGGGTACCATGGGTGGACACAGAATG, PA_r, 5′-CTGTCTTCGCTTTTTAGTCCACAGGAGGAAGACAATGAG, PB_s, 5′-ATTGTCTTCCTCCTGTGGACTAAAAAGCGAAGACAGAGA, PB_r, 5′-GAGCTCGAGTCACTGGGTTATAAATTC.

In Vivo Experiments—For the experimental endotoxemia studies (approved by the Danish Animal Welfare Committee), C57BL/6 mice were injected intravenously with 2.5 mg/kg of LPS (0111:B4, Sigma-Aldrich) in the tail vein. Blood sampling was done under isoflurane anesthesia by orbital bleeding at 0, 30, 60, 120, or 240 min after injection. Serum was collected by centrifugation (3000 g, 20 min) of coagulated blood and analyzed for TNF-α and sCD163 as described. WT C57BL/6 mice were obtained from Taconic (Ry, Denmark). ADAM17$^{ex/ex}$ (26) and *Cd163*$^{-/-}$ (18) mice have been described previously. All mice were maintained at conventional conditions with water and food *ad libitum*.

Statistical Analysis—To analyze the effect of PMA stimulation or amino acid mutations on shedding, Student's *t* test was performed to test for significance between means. Differences were considered significant if $p < 0.05$.

RESULTS

A progressive protein alignment algorithm was used to compare the juxtamembrane sequences of human CD163 and human proTNF-α (Fig. 1*A*); this identified a palindromic sequence consisting of ^{78}Arg-Ser-Ser-Ser-Arg situated next to the ADAM17 cleavage site in proTNF-α (^{76}A ↓ V) and a similar palindrome, ^{1044}Arg-Ser-Ser-Arg, in CD163. A cross-species protein alignment revealed that the Arg-Ser-Ser-Ser-Arg sequence is rather well conserved in the juxtamembrane region of proTNF-α (Fig. 1*B*), whereas the Arg-Ser-Ser-Arg sequence is only present in human and monkey CD163 (Fig. 1*C*). The Arg-Ser-(Ser)-Ser-Arg sequences both in proTNF-α (all species) and in human and monkey CD163 are preceded by a small hydrophobic residue, which in TNF-α represents the final N-terminal residue. A distance-based phylogenetic tree based on the cross-species alignment of the juxtamembrane region of CD163 (Fig. 1*C*) showed a high sequence identity within groups of primates, domestic animals, and rodents.

The importance of the Arg-Ser-Ser-Arg sequence in PMA-induced cleavage of hCD163 was analyzed by comparing the PMA-induced shedding of CD163 in HEK293 cells expressing either wild type hCD163 or the hCD163 ^{1044}RS/AA and ^{1046}SR/AA mutants (Fig. 2, *A* and *C*). The mutants were expressed at the cell surface at comparable levels to wild type hCD163. When we incubated HEK293 cells expressing hCD163 with PMA, the level in the medium increased several-fold to ~9 μg/ml (Fig. 2*C*). In contrast, both the constitutive soluble CD163 release and the PMA-induced release from HEK293 cells expressing hCD163 ^{1044}RS/AA were greatly reduced. Release of sCD163 was also inhibited in HEK293 cells expressing the hCD163 ^{1046}SR/AA mutant, although to a lower extent. This indicates that the entire Arg-Ser-Ser-Arg motif is essential for efficient cleavage, albeit the initial Arg-Ser dipeptide seems particularly important. Inhibition of PMA-induced shedding is also observed when introducing the RS/AA mutation in proTNF-α (proTNF-α ^{78}RS/AA) (Fig. 2, *B* and *D*). Incubation of HEK293 cells expressing proTNF-α with PMA resulted in highly increased TNF-α levels. However, despite similar surface expression of proTNF-α ^{78}RS/AA and wild type proTNF-α, no increase of TNF-α is measured in the medium when incubating HEK293 cells expressing proTNF-α ^{78}RS/AA with PMA (Fig. 2*D*). Interestingly, introduction of the RS/AA mutation inhibits both the constitutive and the PMA-induced shedding in CD163, whereas only the PMA-induced shedding is affected when the RS/AA mutation is introduced in proTNF-α (Fig. 2, *B* and *D*).

To establish whether CD163 is shed in mice, the sCD163 level in mouse serum was estimated by an ELISA specific for

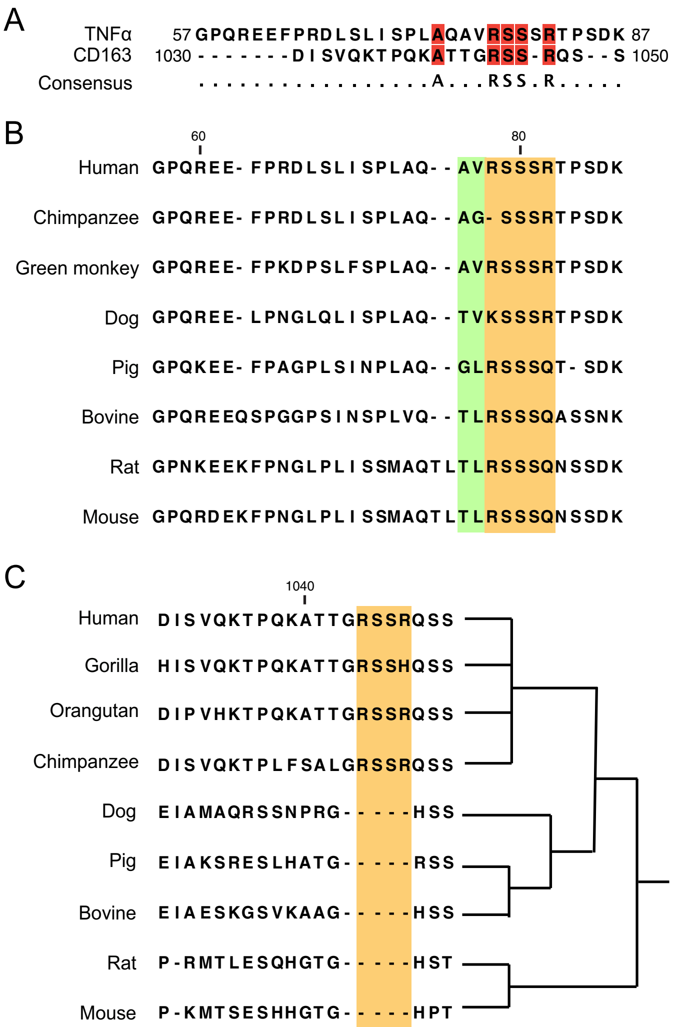

FIGURE 1. **Multiple sequence alignment of CD163 and TNF-α.** *A*, alignment of the human CD163 (amino acids 1030–1050) and the human proTNF-α (amino acids 57–87) juxtamembrane sequences. Identical amino acids are marked in *red*. *B* and *C*, cross-species alignment of the TNF-α juxtamembrane sequence (*B*) and of the CD163 juxtamembrane sequence (*C*). The ADAM17 cleavage site in TNF-α is marked in *green*, and the palindromic Arg-Ser-(Ser)-Ser-Arg sequence is marked in *orange*. All alignments were done in CLC Main Workbench version 6.8.1 using standard gap cost settings (gap open cost: 10.0 and gap extension cost: 1.0).

mouse CD163 (Fig. 3). The concentration of sCD163 in naive mice was ~300 ng/ml, whereas no sCD163 was detected in *Cd163*$^{-/-}$ mice (Fig. 3*A*). To analyze the effect of LPS on sCD163 serum concentration in mice, an experimental endotoxemia study was performed (Fig. 3*B*). Mice received an LPS bolus (2.5 mg/kg) intravenously in the tail vein, and serum concentrations of both sCD163 and TNF-α were monitored over a 240-min time period. As expected, a considerable increase in the TNF-α level was observed after 60 min followed by a fast clearance with no detectable TNF-α after 240 min. In contrast, no change in serum concentration of sCD163 was observed at any of the analyzed time points. To investigate the involvement of ADAM17 in shedding of mouse CD163, the experimental endotoxemia study was repeated in hypomorphic ADAM17$^{ex/ex}$ mice, which exhibit over 95% reduction in ADAM17 expression (26). Challenging ADAM17$^{wt/wt}$ and ADAM17$^{ex/ex}$ mice with LPS resulted in a strong release of TNF-α to the circulation in ADAM17$^{wt/wt}$ mice, whereas no detectable levels of TNF-α were measurable in ADAM$^{ex/ex}$ mice (Fig. 3*C*), highlighting that proinflammatory shedding of TNF-α solely depends on ADAM17 activation. Opposed to this, comparable levels of sCD163 were detected in plasma of both ADAM17$^{wt/wt}$ and ADAM17$^{ex/ex}$ mice after LPS challenge (Fig. 3*D*).

Analysis of LPS-induced shedding of CD163 and TNF-α was repeated *in vitro* using MBDMs. MBDMs were maturated by M-CSF, which led to a substantial CD163 expression as verified by image cytometric analysis (Fig. 4*A*). When we incubated MBDMs with LPS, a large increase in TNF-α was detected in the culture medium, whereas no increase was observed in the level of sCD163 (Fig. 4*B*).

To further validate the involvement of the juxtamembrane region in shedding of human CD163, juxtamembrane chimeras were prepared and expressed in HEK293 cells (Fig. 5*A*). The chimeras consisted of either mouse CD163 with the human juxtamembrane region (mCD163hjux) or human CD163 with the mouse juxtamembrane region (hCD163mjux). The chimeras were expressed at the cell surface at either comparable levels (hCD163mjux) or lower levels (mCD163hjux) as compared with the wild type protein (Fig. 5*B* , *panels a* and *b*). Fig. 5, *C* and *D*, show an immunoblot analysis of CD163 shedding after induction with various PMA concentrations. When we exposed HEK293 cells expressing hCD163 to increasing concentrations of PMA, a dose-dependent release of sCD163 was observed (Fig. 5*C*). In contrast, only a very low and dose-independent release of sCD163 observed when incubating HEK293 cells expressing hCD163mjux with increasing PMA concentrations. However, in HEK293 cells expressing either mCD163 or mCD163hjux, only mCD163hjux-expressing cells displayed a PMA dose-dependent release of sCD163 (Fig. 5*D*). Interestingly, preincubation of the transfected cells with TIMP3, an ADAM17 inhibitor, inhibited the PMA-induced release of hCD163 and mCD163hjux (Fig. 5, *E* and F) The effect of hCD163 juxtamembrane sequence on shedding of mouse CD163 was further investigated using chimeras (mCD163chim1–4) consisting of mouse CD163 substituted with varying length of human CD163 (Fig. 6*A*). PMA-induced and TIMP3-inhibited release of sCD163 was only observed in chimeras containing the human CD163 juxtamembrane region (Fig. 6, *C* and *D*). This also included mCD163chim2, which showed a lower CD163 surface expression as compared with wild type mCD163 and mCD163 chimeras (Fig. 6, *B* and *C*).

Having established a positive effect of the human CD163 juxtamembrane region on shedding of mouse CD163, the importance of the Arg-Ser-Ser-Arg sequence was analyzed by introducing this specific motif next to the conserved Thr-Gly dipeptide in the juxtamembrane region of mouse CD163 (Fig. 7*A*). Introduction of the Arg-Ser-Ser-Arg sequence in mouse CD163 did not change the surface expression of CD163 (Fig. 7*B*). Instead, the 4-amino acid insert induced a PMA-stimulated and TIMP3-inhibited release of mouse sCD163 (Fig. 7, *C* and *D*). When we transfected mCD163 RSSR-expressing HEK293 cells with siRNA against ADAM17, the mRNA level of ADAM17 was reduced to ~60% of controls (Fig. 7*E*), which resulted in an inhibition of the PMA-induced release of sCD163 (Fig. 7*F*).

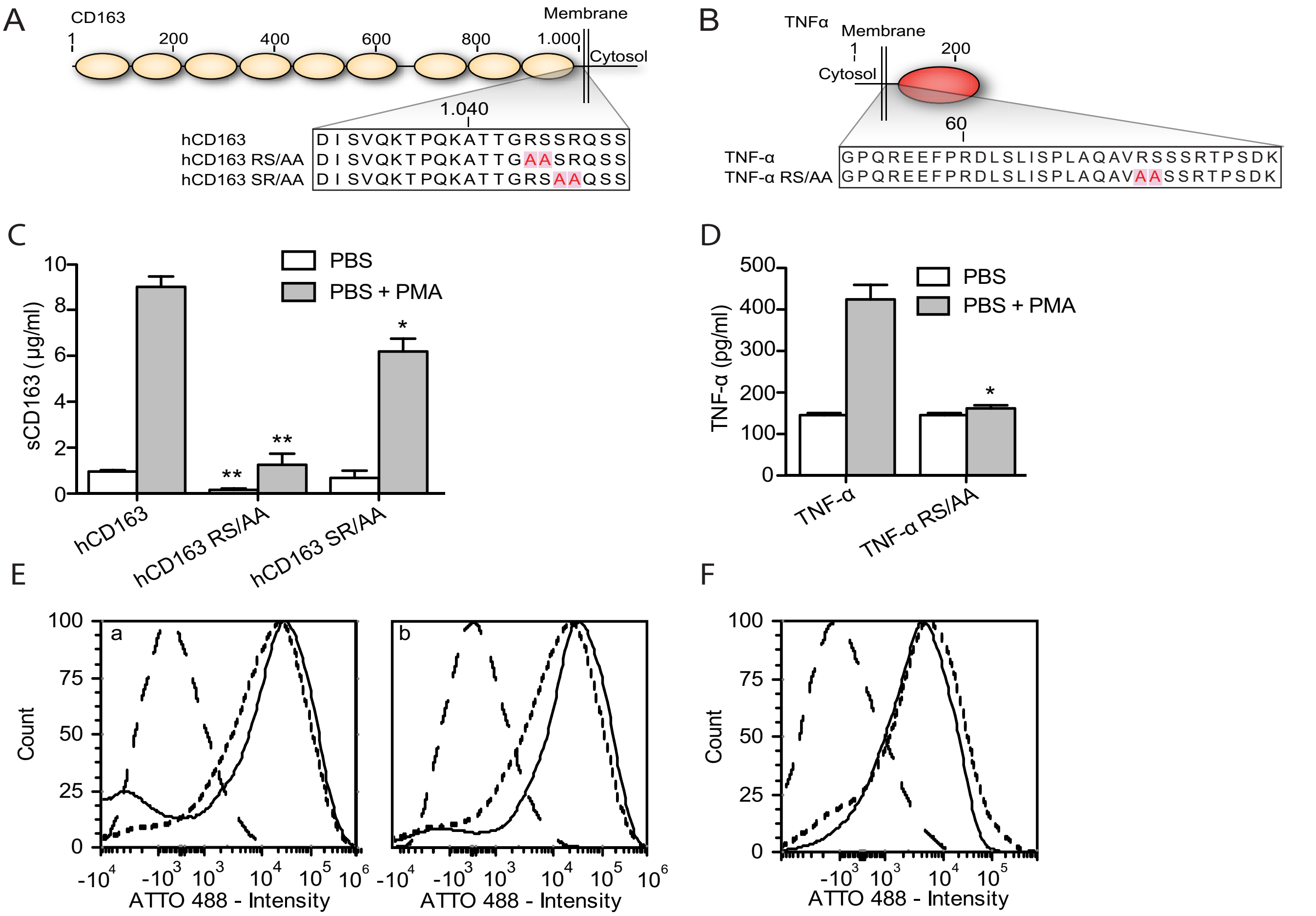

FIGURE 2. **PMA-induced release of sCD163 and TNF-α from HEK293 cells expressing CD163 and proTNF-α RSXSR mutants.** *A* and *B*, overview of CD163 and proTNF-α Arg-Ser-(Ser)-Ser-Arg mutants. *C* and *D*, ELISA measurements of sCD163 (*C*) or TNF-α (*D*) in media from cells stimulated with (*PBS + PMA*) or without PMA (*PBS*). Data represent mean ± S.E. of three individual experiments. *Asterisks* denote a mean significant difference from wild type protein under similar conditions (*, $p < 0.01$; **, $p < 0.001$ in Student's *t* test). *E* and *F*, image cytometric analysis of CD163 (*E*) or TNF-α expression (*F*) in HEK293 cells using either mouse mAb anti-human CD163 IgG (Mac2-158) or mouse mAb anti-human TNF-α IgG and ATTO488-labeled rabbit pAb anti-mouse IgG. The *dashed line* represents mock-transfected control, the *dotted line* represents cells expressing hCD163 (*E*) or TNF-α (*F*), and the *solid line* represents cells expressing hCD163 RS/AA (*E, panel a*), hCD163 SR/AA (*E, panel b*), or TNF-α RS/AA (*F*).

DISCUSSION

In the present study, we have demonstrated that a palindromic sequence (Arg-Ser-(Ser)-Ser-Arg) present in both human CD163 and TNF-α is necessary for an efficient ADAM17-mediated cleavage. Mutation of the palindromic sequence in human CD163 affected both the induced and the constitutive release of sCD163, which corresponds with earlier findings suggesting that ADAM17 functions as both a constitutive and an inducible sheddase of CD163 (7). Cross-species sequence alignment of the juxtamembrane region in CD163 revealed that species other than primates completely lacked the Arg-Ser-(Ser)-Ser-Arg sequence. In line with this, we show that despite the existence of sCD163 in mouse serum, the protein is not released to the circulation via ADAM17-mediated cleavage. Importantly, we were able to verify the importance of the Arg-Ser-Ser-Arg sequence by enabling ADAM17-mediated shedding in mouse CD163 using chimeras of mouse CD163 including the human juxtamembrane sequence or the Arg-Ser-Ser-Arg sequence.

So far, more than 75 different proteins (2) have been identified as substrates for ADAM17. Despite the vast number of proteins, no consensus sequence for ADAM17-mediated proteolysis has been identified, and therefore it seems obvious that ADAM17 may cleave in rather variant sequences. Screening of peptide libraries has shown a prevalence of small hydrophobic residues at the substrate P1′ position, basic residues at P2′, and small aliphatic residues at P3′, although with weaker selectivity (27). Recently, it was also reported that the ADAM17 activity relied on the secondary structure of the substrate and other noncatalytic domains in the enzyme (28). The present findings comply with the P1′-P3′ consensus rule in the sense that the Arg-Ser-(Ser)-Ser-Arg sequence in both proTNF-α and CD163 is preceded by a small hydrophobic residue (P1′ position). Arg and Ser in the tetrapeptide then represent the basic and small aliphatic residue at P2′ and P3′, respectively. As such, It is possible that the a small hydrophobic residue followed by Arg-Ser-(Ser)-Ser-Arg represents an optimized sequence for ADAM17-mediated cleavage. However, it should be noted that exact Arg-Ser-(Ser)-Ser-Arg motifs are absent from most proteins known to be cleaved by ADAM17, and the motif is therefore not a prerequisite for ADAM17-mediated cleavage.

N-terminal sequencing has identified Val-Arg-Ser-Ser-Ser-Arg as the N terminus of TNF-α, whereas the precise cleavage

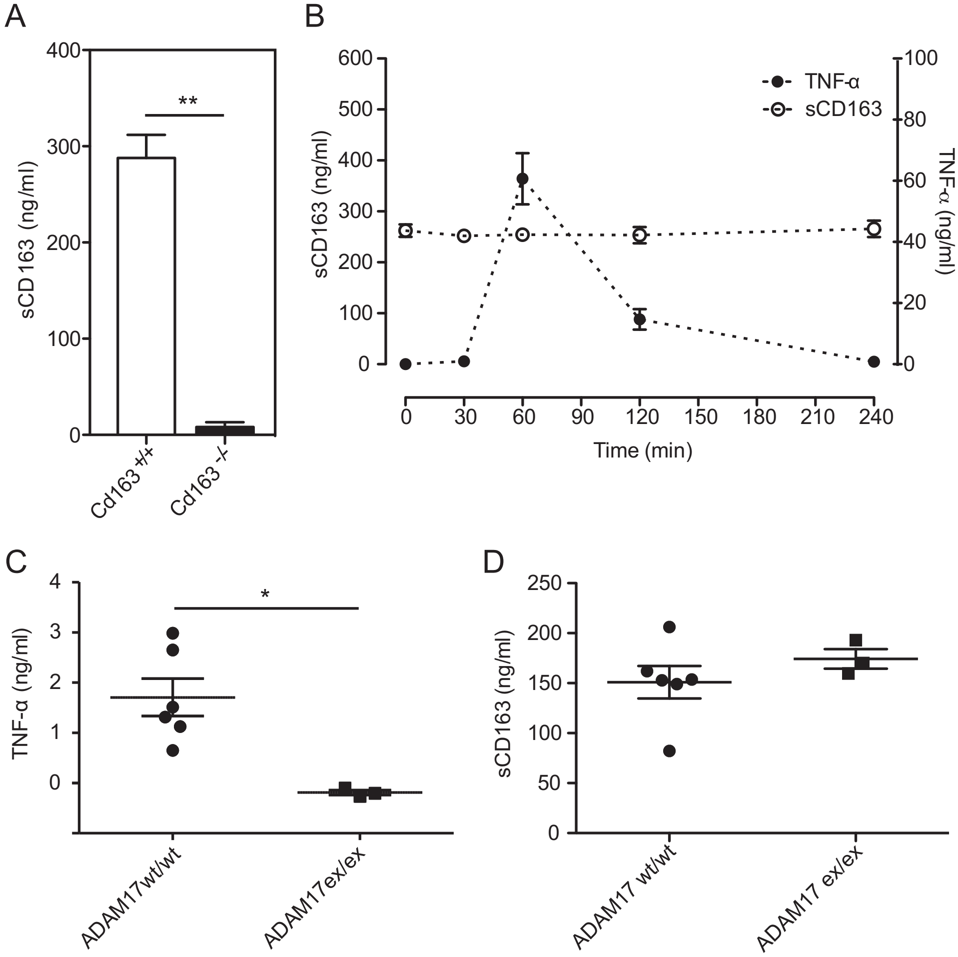

FIGURE 3. **Release of sCD163 and TNF-α during endotoxemia in wild type and ADAM17$^{ex/ex}$ mice.** *A*, ELISA measurement of sCD163 in mouse sera from C57BL/6NTac wild type (*Cd163*$^{+/+}$) and CD163 knock-out (*Cd163*$^{-/-}$) mice. *B*, levels of sCD163 and TNF-α in mouse sera ($n = 4$) after an intravenous bolus injection of LPS in the tail vein. Levels of sCD163 and TNF-α were measured by ELISA in sera collected at 0, 30, 60, 120, and 240 min after LPS injection. *C* and *D*, ELISA measurements of TNF-α (*C*) and sCD163 (*D*) in sera from ADAM17$^{wt/wt}$ ($n = 6$) and ADAM17$^{ex/ex}$ ($n = 3$) mice. Serum was collected 60 min after an intravenous bolus injection of LPS. Data represent mean ± S.E. of three individual experiments. *Asterisks* denote a mean significant difference between groups (*, $p < 0.01$; **, $p < 0.0001$ in Student's *t* test).

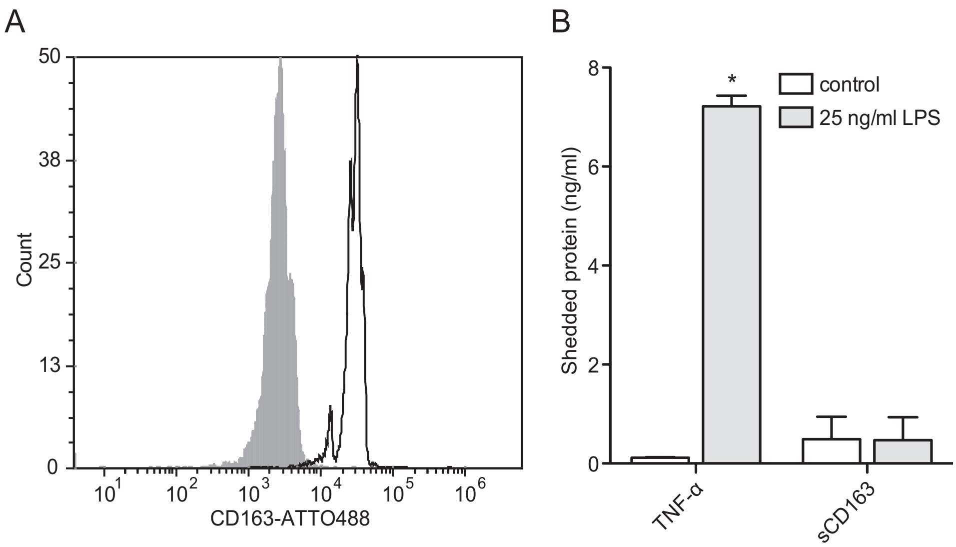

FIGURE 4. **LPS-induced shedding of CD163 and TNF-α in MBDMs.** *A*, image cytometric analysis of CD163 expression on MBDMs using rabbit ATTO488-labeled pAb anti-mouse CD163 IgG (*white*) and ATTO488-labeled rabbit IgG (*gray*) as control. *B*, release of TNF-α and sCD163 from MBDMs incubated with LPS for 4 h in complete medium was measured using ELISA. Data represent mean ± S.E. of three separate experiments. An *asterisk* denotes a mean significant difference from untreated control ($p < 0.0001$ in Student's *t* test).

site of CD163 is unknown. However, the P1′-P3′ consensus rule and the present data including the knock-in data in mouse CD163 indicate that cleavage may occur between Thr[1042] and Gly[1043]. (Fig. 8). However, because CD163 is a type I transmembrane protein, which is cleaved in the C terminus, the [1043]Gly-Arg-Ser-Ser-Arg motif will not, as in the case of proTNF-α,

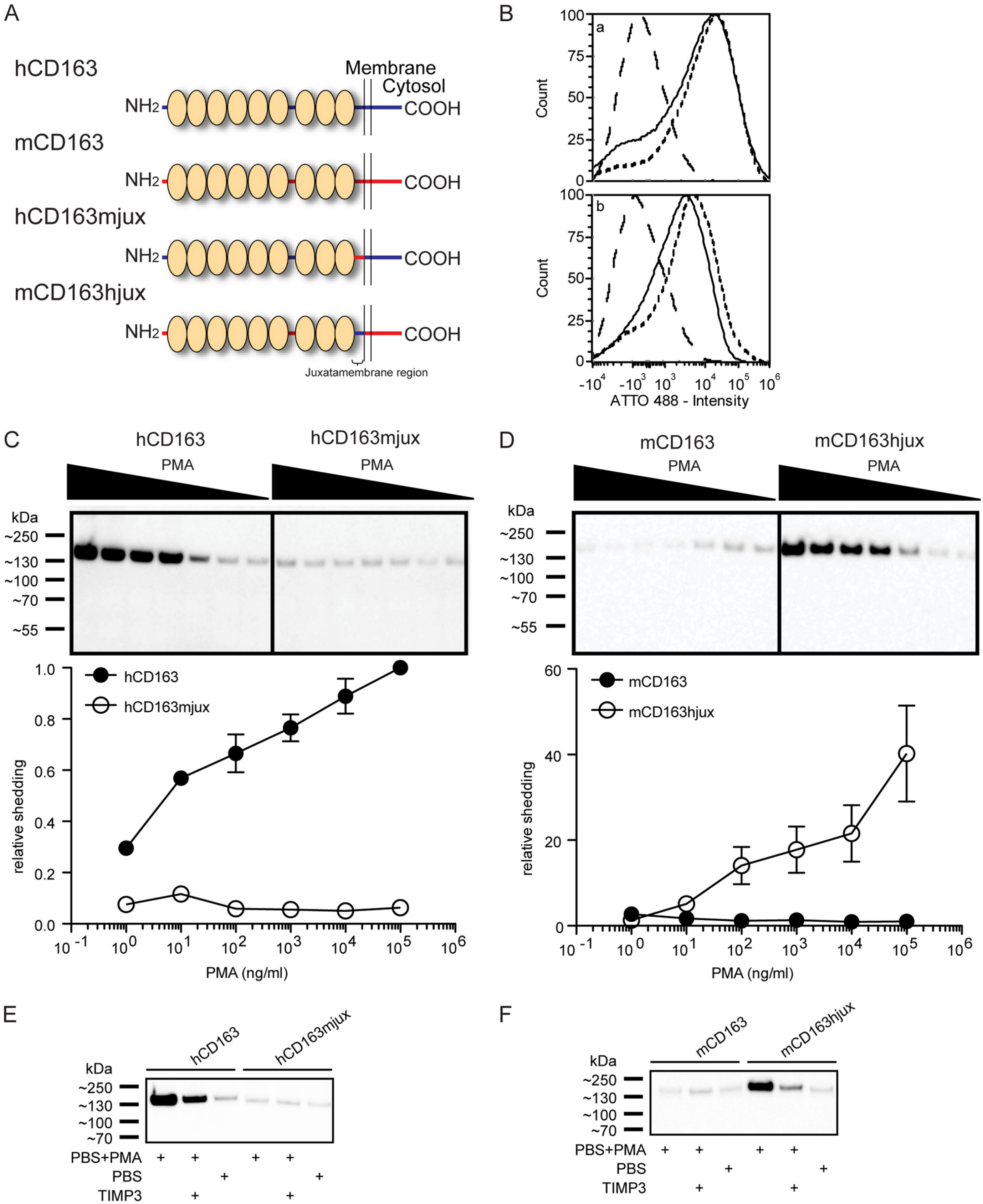

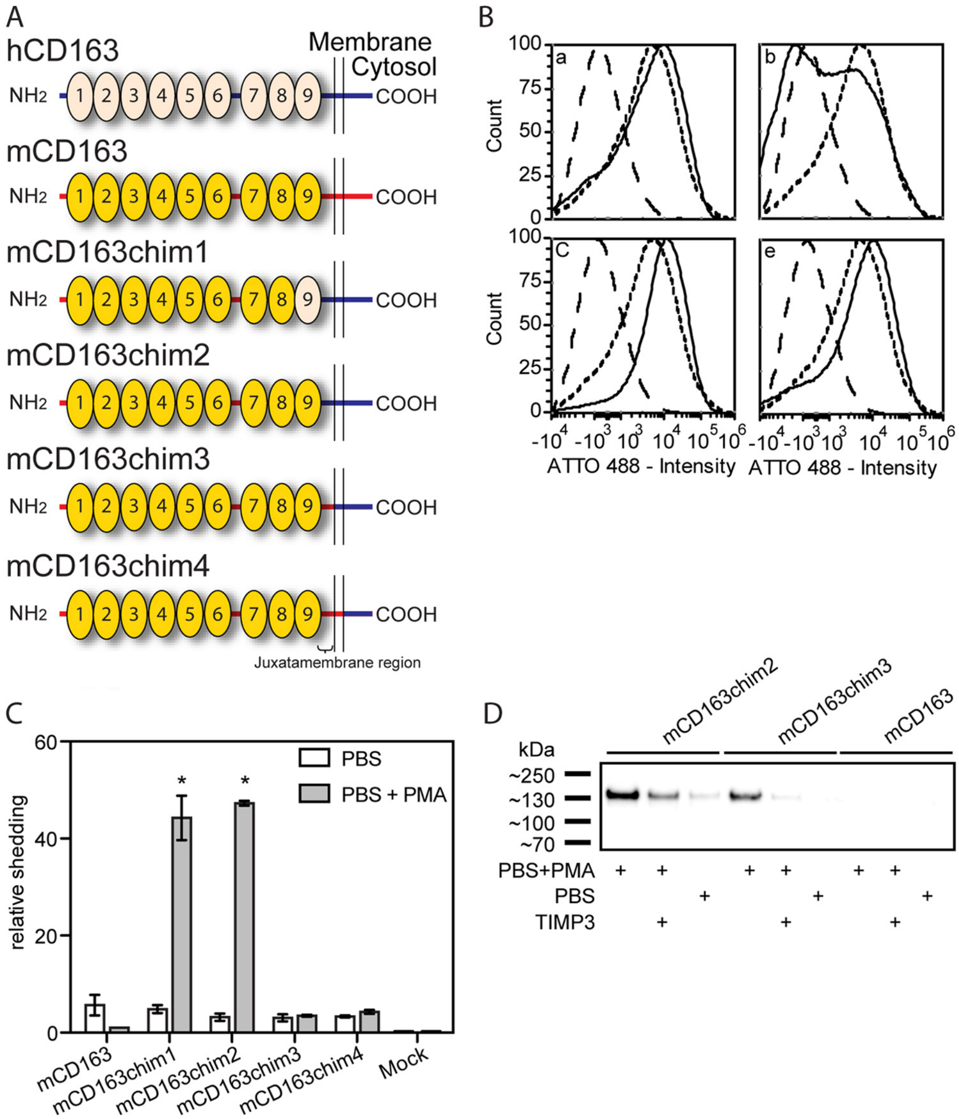

FIGURE 6. **PMA-induced release of CD163 in HEK293 cells expressing mouse CD163 substituted with varying parts of human CD163.** *A*, domain structure of CD163 chimeras. The human CD163 sequence is shown in *blue*, and the human SRCR domains are in *light orange*. The mouse CD163 sequence is displayed in *red*, and the mouse SRCR domains are displayed in *yellow*. *B*, image cytometric analysis of CD163 expression in HEK293 cells using rabbit pAb anti-mouse CD163-ATTO488. The *dashed line* represents mock-transfected control, the *dotted line* represents cells expressing mCD163, and the *solid line* represents cells expressing mCD163chim1 (*panel a*), mCD163chim2 (*panel b*), mCD163chim3 (*panel c*), or mCD163chim4 (*panel d*). *C*, relative release of sCD163 from HEK293 cells expressing human/mouse CD163 chimeras. Shedding is relative to release of sCD163 from PMA-incubated HEK293 cells expressing mCD163. Levels of sCD163 in the supernatant of unstimulated (*PBS*) and PMA-stimulated cells (*PBS + PMA*) was measured by immunoblot analysis. Immunoreactive bands were visualized by rabbit pAb anti-mouse CD163 and HRP-conjugated goat anti-rabbit IgG. Band intensities were subsequently quantified using the MultiGauge software (Fujifilm Europe). An *asterisk* denotes a mean significant difference from untreated control ($p < 0.0001$). Data represent mean ± S.E. of three individual experiments. *D*, Western blot analysis of sCD163 release from CD163-transfected HEK293 cells incubated with PMA and TIMP3 inhibitor. Immunoreactive bands were visualized using rabbit pAb anti-mouse CD163 and HRP-conjugated goat anti-rabbit IgG.

represent the N terminus of the released soluble product. Instead, this sequence will constitute the N-terminal end of the CD163 receptor stub in the membrane.

ProTNF-α is a type II transmembrane protein, whereas CD163 is a type I transmembrane protein, and as such, they have opposite orientation. The identification of a similar palin-

FIGURE 5. **PMA-induced release of CD163 in HEK293 cells expressing juxtamembrane chimeras of CD163.** *A*, domain structure of CD163 juxtamembrane chimeras. The human CD163 sequence is shown in *blue*, and the mouse CD163 sequence is shown in *red*. *B*, image cytometric analysis of CD163 surface expression using mouse mAb anti-human CD163 IgG (Mac2-158) and goat pAb anti-mouse ATTO488 (*panel a*) or rabbit pAb anti-mouse CD163-ATTO488 (*panel b*). The *dashed line* represents mock-transfected control, the *dotted line* represents cells expressing hCD163 (*panel a*) or mCD163 (*panel b*), and the *solid line* represents cells expressing hCD163mjux (*panel a*) or mCD163hjux (*panel b*). *C* and *D*, Western blot analysis of PMA-induced release of sCD163 from transfected HEK293 cells using a PMA gradient. Immunoreactive bands were visualized using either mouse mAb anti-human CD163 (Mac2-158) and HRP-conjugated goat anti-mouse IgG (*C*) or rabbit pAb anti-mouse CD163 and HRP-conjugated goat anti-rabbit IgG (*D*). Band intensities were estimated using the MultiGauge software (Fujifilm Europe), and relative shedding was calculated and plotted against the PMA concentration. Shedding is relative to the band intensity of released sCD163 from HEK293 cells expressing either hCD163 (*C*) or mCD163 (*D*) incubated with 10^5 ng/ml PMA. Data represent mean ± S.E. of three individual experiments. *E* and *F*, Western blot analysis of sCD163 release from transfected HEK293 cells incubated with PMA and TIMP3 inhibitor. Immunoreactive bands were visualized using either mouse mAb anti-human CD163 (Mac2-158) and HRP-conjugated goat anti-mouse IgG (*E*) or rabbit pAb anti-mouse CD163 and HRP-conjugated goat anti-rabbit IgG (*F*).

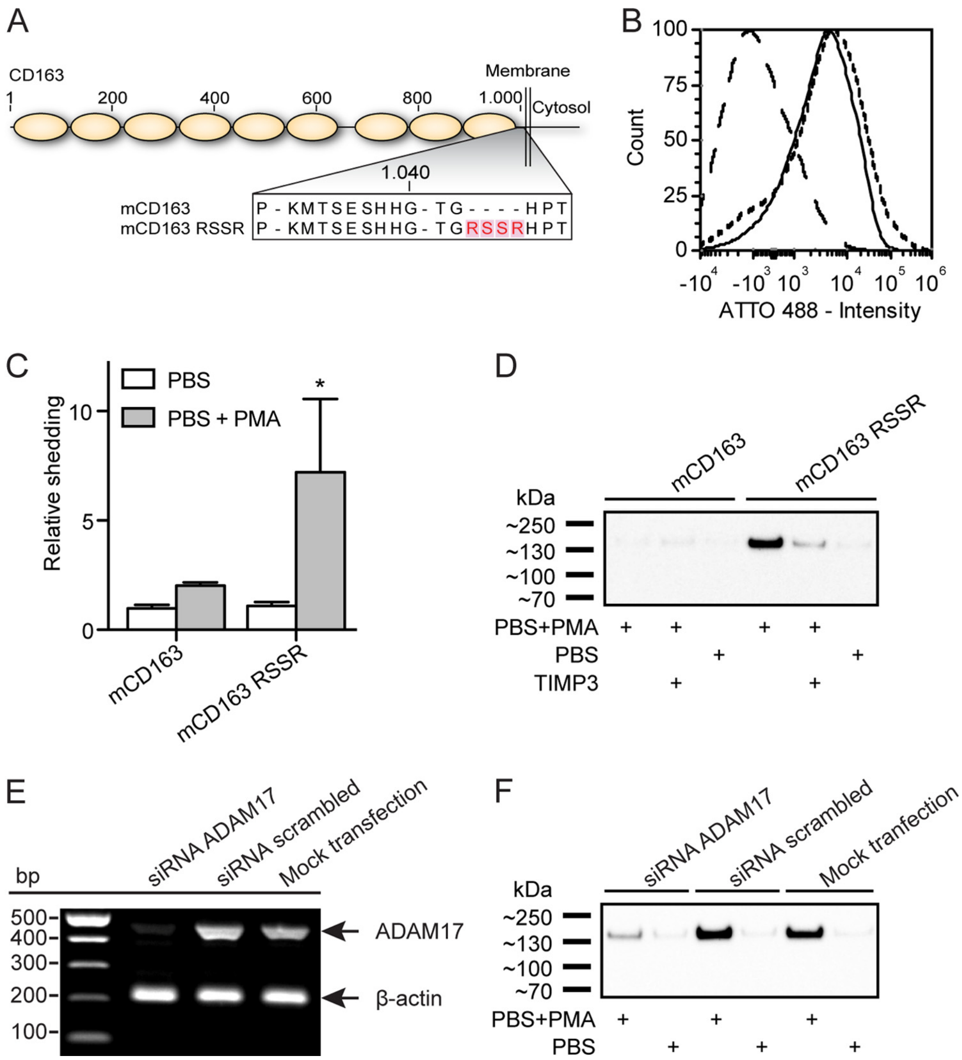

FIGURE 7. **PMA efficiently induces an ADAM17-dependent release of CD163 in HEK293 cells expressing mouse CD163 containing the Arg-Ser-Ser-Arg sequence.** *A*, sequence of mCD163 and mCD163 RSSR mutant. *B*, image cytometric analysis of CD163 expression in HEK293 cells using rabbit pAb anti-mouse CD163-ATTO488. The *dashed line* represents mock-transfected control, the *dotted line* represents cells expressing mCD163, and the *solid line* represents cells expressing mCD163-RSSR. *C*, relative release of sCD163 from HEK293 cells expressing the mouse CD163 or mouse CD163 RSSR mutant. Shedding is relative to release of sCD163 from PMA-incubated HEK293 cells expressing mCD163. Levels of sCD163 in supernatant of unstimulated (*PBS*) and PMA-stimulated cells (*PBS* + *PMA*) were measured by immunoblot analysis. Immunoreactive bands were visualized using rabbit pAb anti-mouse CD163 and HRP-conjugated goat anti-rabbit IgG. The intensities of the immunoreactive bands were subsequently quantified using the MultiGauge software (Fujifilm Europe). An *asterisk* denotes a mean significant difference from wild type protein under similar conditions ($p < 0.05$). Data represent mean ± S.E. of three individual experiments. *D*, Western blot analysis of sCD163 release from CD163-transfected HEK293 cells incubated with PMA and TIMP3 inhibitor. Immunoreactive bands were visualized using rabbit pAb anti-mouse CD163 and HRP-conjugated goat anti-rabbit IgG. *E*, semiquantitative RT-PCR analysis of gene-specific siRNA silencing of ADAM17 in mouse CD163 RSSR-expressing HEK293 cells, which were either mock-transfected or transfected with siRNA against ADAM17 or scrambled siRNA. Cells were harvested 48 h after transfection and subjected to RT-PCR analysis using β-actin as control. *F*, Western blot analysis of sCD163 release from siRNA-transfected HEK293 cells expressing the mouse CD163 RSSR mutant. Immunoreactive bands were visualized using rabbit pAb anti-mouse CD163 and HRP-conjugated goat anti-rabbit IgG.

dromic sequence important for ADAM17-mediated cleavage in opposite oriented substrates could suggest a parallel to palindromic sequences known from DNA restriction enzymes. However, palindromic peptide sequences are not identical structures in both directions due to the unidirectional orientation of the carboxyl and amino groups involved in the peptide bonds. Consequently, both proTNF-α and CD163 have to present the Arg-Ser-(Ser)-Ser-Arg sequence to the membrane-associated ADAM17 in the same orientation. Flexibility of the juxtamembrane regions in CD163 or proTNF-α may allow the right orientation for recognition by ADAM17. Alternatively, high flexibility of the extracellular domain of ADAM17 could also allow recognition of the motif in either orientation.

In the present study, we have shown that mouse CD163 lacks the ability to undergo ADAM17-dependent shedding, although sCD163 is easily detectable in mouse serum. So far, it is not known whether mouse sCD163 is released via regulated proteolysis or merely as a byproduct of macrophage turnover. Recently, it was shown that another human ADAM17 substrate, the interleukin-6 receptor, was not shed by this enzyme in mice (29). Instead, the substrate was shed by the closely related ADAM10, which only had minimal activity toward the substrate in humans. One could also speculate that CD163 in mouse serum is an uncleaved receptor present in macrophage-released exosomes, as has been shown for the structurally related protein CD163-L1 in humans (30). Given the relatively

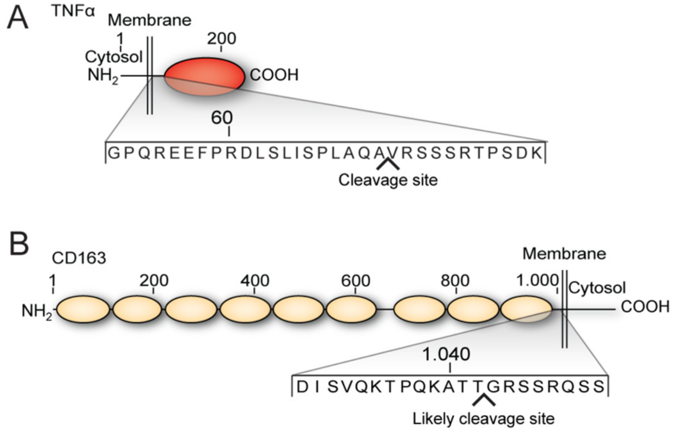

FIGURE 8. **Predicted ADAM17 cleavage site in human CD163.** *A*, overview of the type II transmembrane protein proTNF-α highlighting the ADAM17 cleavage site identified in the 31-amino acid juxtamembrane region (6). *B*, overview of the human type I membrane protein CD163 highlighting the likely ADAM17 cleavage site in the 21-amino acid juxtamembrane region.

high level of sCD163 in mouse and human plasma, it is possible that a common basal level of exosome-associated CD163 exists in both species and that humans under inflammatory conditions are able to increase the concentration of the receptor in plasma by ADAM17-dependent release of sCD163.

Interestingly, the striking difference in human and mouse CD163 in terms of ADAM17-mediated cleavage parallels a number of other differences in the function of primate haptoglobins *versus* the haptoglobins in non-primates. One example is the primate-specific defense mechanism against trypanosome parasites. Here, the primate-specific haptoglobin gene duplication product, haptoglobin-related protein, binds together with another primate-specific protein, apolipoprotein-L1, to exert a trypanolytic function (15). Another example is our recent finding that human haptoglobin upon complex formation with hemoglobin has a much higher affinity for CD163 than mouse haptoglobin in complex with hemoglobin (18). In return, mouse free hemoglobin binds with higher affinity to CD163 as compared with human hemoglobin. Apparently, the difference in affinity between haptoglobin-hemoglobin complexes in the two species relies on a primate-specific presence of two basic residues in a haptoglobin loop that interacts with CD163 when haptoglobin is complexed to hemoglobin (31). A third example, the plasma concentration of haptoglobin, is generally much higher in primates *versus* in non-primates (32, 33).

The serious threat of trypanosome parasites causing sleeping sickness most likely may have driven the evolution of resistance toward certain types of trypanosome parasites by means of primate-specific haptoglobin-related protein and apolipoprotein-L. It is tempting to speculate that other infectious diseases such as malaria or other hemolytic infections may also have caused an evolutionary pressure leading to development of additional protection by haptoglobin. However, the increased protection obtained by higher concentrations of haptoglobin and a faster CD163-mediated clearance of haptoglobin-hemoglobin complexes may lead to an inexpedient overdamping of the inflammatory response induced by anti-inflammatory heme metabolites. Hence, an ADAM17-dependent mechanism to down-regulate CD163 expression in primates may have evolved to tune the system and thereby achieve the right balance between protection from hemolysis and overdamping of the proinflammatory response.

REFERENCES

1. Gooz, M. (2010) ADAM-17: the enzyme that does it all. *Crit. Rev. Biochem. Mol. Biol.* **45,** 146–169
2. Scheller, J., Chalaris, A., Garbers, C., and Rose-John, S. (2011) ADAM17: a molecular switch to control inflammation and tissue regeneration. *Trends Immunol.* **32,** 380–387
3. Moss, M. L., Jin, S. L., Milla, M. E., Bickett, D. M., Burkhart, W., Carter, H. L., Chen, W. J., Clay, W. C., Didsbury, J. R., Hassler, D., Hoffman, C. R., Kost, T. A., Lambert, M. H., Leesnitzer, M. A., McCauley, P., McGeehan, G., Mitchell, J., Moyer, M., Pahel, G., Rocque, W., Overton, L. K., Schoenen, F., Seaton, T., Su, J. L., and Becherer, J. D. (1997) Cloning of a disintegrin metalloproteinase that processes precursor tumour-necrosis factor-α. *Nature* **385,** 733–736
4. Black, R. A., Rauch, C. T., Kozlosky, C. J., Peschon, J. J., Slack, J. L., Wolfson, M. F., Castner, B. J., Stocking, K. L., Reddy, P., Srinivasan, S., Nelson, N., Boiani, N., Schooley, K. A., Gerhart, M., Davis, R., Fitzner, J. N., Johnson, R. S., Paxton, R. J., March, C. J., and Cerretti, D. P. (1997) A metalloproteinase disintegrin that releases tumour-necrosis factor-α from cells. *Nature* **385,** 729–733
5. Horiuchi, K., Kimura, T., Miyamoto, T., Takaishi, H., Okada, Y., Toyama, Y., and Blobel, C. P. (2007) Cutting edge: TNF-α-converting enzyme (TACE/ADAM17) inactivation in mouse myeloid cells prevents lethality from endotoxin shock. *J. Immunol.* **179,** 2686–2689
6. Wang, A. M., Creasey, A. A., Ladner, M. B., Lin, L. S., Strickler, J., Van Arsdell, J. N., Yamamoto, R., and Mark, D. F. (1985) Molecular cloning of the complementary DNA for human tumor necrosis factor. *Science* **228,** 149–154
7. Etzerodt, A., Maniecki, M. B., Møller, K., Møller, H. J., and Moestrup, S. K. (2010) Tumor necrosis factor α-converting enzyme (TACE/ADAM17) mediates ectodomain shedding of the scavenger receptor CD163. *J. Leukoc Biol.* **88,** 1201–1205
8. Otterbein, L. E., Soares, M. P., Yamashita, K., and Bach, F. H. (2003) Heme oxygenase-1: unleashing the protective properties of heme. *Trends Immunol.* **24,** 449–455
9. Thomsen, J. H., Etzerodt, A., Svendsen, P., and Moestrup, S. K. (2013) The haptoglobin-CD163-heme oxygenase-1 pathway for hemoglobin scavenging. *Oxid. Med. Cell. Longev.* **2013,** 523652
10. Etzerodt, A., and Moestrup, S. K. (2013) CD163 and INFLAMMATION: Biological, diagnostic, and therapeutic aspects. *Antioxid. Redox. Signal.* **18,** 2352–2363
11. Møller, H. J., Nielsen, M. J., Maniecki, M. B., Madsen, M., and Moestrup, S. K. (2010) Soluble macrophage-derived CD163: a homogenous ectodomain protein with a dissociable haptoglobin-hemoglobin binding. *Immunobiology* **215,** 406–412
12. Møller, H. J., Peterslund, N. A., Graversen, J. H., and Moestrup, S. K. (2002) Identification of the hemoglobin scavenger receptor/CD163 as a natural soluble protein in plasma. *Blood* **99,** 378–380
13. Møller, H. J. (2012) Soluble CD163. *Scand. J. Clin. Lab. Invest.* **72,** 1–13
14. Weaver, L. K., Hintz-Goldstein, K. A., Pioli, P. A., Wardwell, K., Qureshi, N., Vogel, S. N., and Guyre, P. M. (2006) Pivotal advance: activation of cell surface Toll-like receptors causes shedding of the hemoglobin scavenger receptor CD163. *J. Leukoc. Biol.* **80,** 26–35
15. Vanhollebeke, B., De Muylder, G., Nielsen, M. J., Pays, A., Tebabi, P., Dieu, M., Raes, M., Moestrup, S. K., and Pays, E. (2008) A haptoglobin-hemoglobin receptor conveys innate immunity to *Trypanosoma brucei* in humans. *Science* **320,** 677–681
16. Högger, P., and Sorg, C. (2001) Soluble CD163 inhibits phorbol ester-induced lymphocyte proliferation. *Biochem. Biophys. Res. Commun.* **288,** 841–843
17. Kneidl, J., Löffler, B., Erat, M. C., Kalinka, J., Peters, G., Roth, J., and Barczyk, K. (2012) Soluble CD163 promotes recognition, phagocytosis and killing of *Staphylococcus aureus* via binding of specific fibronectin pep-

tides. *Cell. Microbiol.* **14,** 914–936

18. Etzerodt, A., Kjolby, M., Nielsen, M. J., Maniecki, M., Svendsen, P., and Moestrup, S. K. (2013) Plasma clearance of hemoglobin and haptoglobin in mice and effect of CD163 gene targeting disruption. *Antioxid. Redox. Signal.* **18,** 2254–2263
19. Kristiansen, M., Graversen, J. H., Jacobsen, C., Sonne, O., Hoffman, H. J., Law, S. K., and Moestrup, S. K. (2001) Identification of the haemoglobin scavenger receptor. *Nature* **409,** 198–201
20. Etzerodt, A., Maniecki, M. B., Graversen, J. H., Møller, H. J., Torchilin, V. P., and Moestrup, S. K. (2012) Efficient intracellular drug-targeting of macrophages using stealth liposomes directed to the hemoglobin scavenger receptor CD163. *J. Control. Release* **160,** 72–80
21. Manzanero, S. (2012) Generation of mouse bone marrow-derived macrophages. *Methods Mol. Biol.* **844,** 177–181
22. Møller, H. J., Hald, K., and Moestrup, S. K. (2002) Characterization of an enzyme-linked immunosorbent assay for soluble CD163. *Scand. J. Clin. Lab. Invest.* **62,** 293–299
23. Maniecki, M. B., Etzerodt, A., Moestrup, S. K., Møller, H. J., and Graversen, J. H. (2011) Comparative assessment of the recognition of domain-specific CD163 monoclonal antibodies in human monocytes explains wide discrepancy in reported levels of cellular surface CD163 expression. *Immunobiology* **216,** 882–890
24. Chiu, J., March, P. E., Lee, R., and Tillett, D. (2004) Site-directed, Ligase-Independent Mutagenesis (SLIM): a single-tube methodology approaching 100% efficiency in 4 h. *Nucleic Acids Res.* **32,** e174
25. Wurch, T., Lestienne, F., and Pauwels, P. J. (1998) A modified overlap extension PCR method to create chimeric genes in the absence of restriction enzymes. *Biotechnol. Tech.* **12,** 653–657
26. Chalaris, A., Adam, N., Sina, C., Rosenstiel, P., Lehmann-Koch, J., Schirmacher, P., Hartmann, D., Cichy, J., Gavrilova, O., Schreiber, S., Jostock, T., Matthews, V., Häsler, R., Becker, C., Neurath, M. F., Reiss, K., Saftig, P., Scheller, J., and Rose-John, S. (2010) Critical role of the disintegrin metalloprotease ADAM17 for intestinal inflammation and regeneration in mice. *J. Exp. Med.* **207,** 1617–1624
27. Caescu, C. I., Jeschke, G. R., and Turk, B. E. (2009) Active-site determinants of substrate recognition by the metalloproteinases TACE and ADAM10. *Biochem. J.* **424,** 79–88
28. Stawikowska, R., Cudic, M., Giulianotti, M., Houghten, R. A., Fields, G. B., and Minond, D. (2013) Activity of a disintegrin and metalloprotease 17 (ADAM17) is regulated by its non-catalytic domains and secondary structure of its substrates. *J. Biol. Chem.* **288,** 22871–22879
29. Garbers, C., Jänner, N., Chalaris, A., Moss, M. L., Floss, D. M., Meyer, D., Koch-Nolte, F., Rose-John, S., and Scheller, J. (2011) Species specificity of ADAM10 and ADAM17 proteins in interleukin-6 (IL-6) trans-signaling and novel role of ADAM10 in inducible IL-6 receptor shedding. *J. Biol. Chem.* **286,** 14804–14811
30. Looze, C., Yui, D., Leung, L., Ingham, M., Kaler, M., Yao, X., Wu, W. W., Shen, R.-F., Daniels, M. P., and Levine, S. J. (2009) Proteomic profiling of human plasma exosomes identifies PPARγ as an exosome-associated protein. *Biochem. Biophys. Res. Commun.* **378,** 433–438
31. Nielsen, M. J., Andersen, C. B. F., and Moestrup, S. K. (2013) CD163 binding to haptoglobin-hemoglobin complexes involves a dual-point electrostatic receptor-ligand pairing. *J. Biol. Chem.* **288,** 18834–18841
32. Delanghe, J., Allcock, K., Langlois, M., Claeys, L., and De Buyzere, M. (2000) Fast determination of haptoglobin phenotype and calculation of hemoglobin binding capacity using high pressure gel permeation chromatography. *Clin. Chim. Acta* **291,** 43–51
33. Knyszynski, A., and Burger, M. (1971) Increase of haptoglobin concentration in mouse serum by endotoxin and by a serum factor. *Experientia* **27,** 838–839